Scattering of electromagnetic waves by nearly periodic structures

A. Modinos and V. Yannopapas*
Department of Physics, National Technical University of Athens, Zografou Campus, GR-157 73 Athens, Greece

N. Stefanou
University of Athens, Section of Solid State Physics, Panepistimioupolis, GR-157 84 Athens, Greece
(Received 22 June 1999; revised manuscript received 21 September 1999)

We present a method, based on the coherent potential approximation, for the treatment of disorder in photonic crystals. We apply the method to the study of light absorption by a three-dimensional array of plasma spheres distributed randomly in a host dielectric medium. We find that the effect of disorder on the absorbance of a thick slab of the material consisting of many layers of spheres is much less pronounced than in the corresponding case of a single layer of spheres.

I. INTRODUCTION

In recent years, photonic crystals, i.e., composite materials with a dielectric function that is a periodic function of the position, have attracted much interest, mainly because of the possibility of frequency gaps in such systems, which in turn promises revolutionary applications in optoelectronics.[1–3] For different reasons there has been for many years a lot of interest in the optical properties of energy-absorbing small metallic particles distributed periodically or randomly in a host dielectric medium. Such systems are used, e.g., as coatings for solar energy absorbers.[4–7] The theoretical analysis in this second category is essentially the same as for photonic crystals consisting of dielectric spheres in a medium of different dielectric function. In either case, the problem is much easier to solve for a periodic than for a non-periodic arrangement of spheres.

Most of the theoretical analysis relating to photonic crystals, so far, has been based on the assumption of perfect periodicity.[8–11] And yet it is important to know, what the effect would be of deviation from periodicity on the size of frequency gaps and other important parameters, since real systems are more likely to involve some deviations from periodicity. The actual amount of disorder would depend of course on the type and on the precision of the fabrication technique used.[12,13] Even greater deviations from periodicity are evident in systems of small metallic particles in a dielectric medium since the size, shape, and the distribution of the particles is usually not uniform.[5,14] Some attempts to account for deviations from periodicity in two-dimensional (2D)[15,16] and three-dimensional (3D) structures[17] have already been made but a lot remains to be done.

In the present paper, we develop a formalism for estimating the effect of disorder on the optical properties of a system that consists of nonoverlapping spheres in a host medium. The formalism is based on the so-called single-site coherent potential approximation (CPA), which has been used extensively in the study of the electronic properties of disordered alloys,[18–20] and is expected to give reasonably good results at least in the case of relatively weak disorder. A CPA treatment of disorder has been applied to the study of the optical properties of randomly distributed spheres in a 2D lattice by Persson and Liebsch[21] and in 3D lattices by Liebsch and Persson,[22] in the limit when the electrostatic approximation is valid (the interparticle distance is much smaller than the wavelength of light, and the fractional volume occupied by the spheres is relatively small). Two of us[15] presented a CPA treatment of light scattering by a disordered 2D array of nonoverlapping spheres, which remains valid for any frequency of the incident light and for any concentration of the spheres. In the present work we extend the method presented in Ref. 15 to a 3D array of spheres. This is done in Sec. II. The numerical implementation of the formalism and some technical aspects of the computation are discussed in Sec. III. In Sec. IV we use our method to study the absorption of light by a finite slab consisting of metallic particles (plasma spheres) distributed randomly in a host dielectric medium. We compare the above quantity with the corresponding one for a periodic structure. Moreover, we compare the effects of disorder in 3D systems with the effect of the same in 2D systems.

II. THEORY

A. The Model

In general, the system we are considering consists of a number of planes of nonoverlapping spheres parallel to the xy plane. We refer to it as a slab. The spheres of the νth plane belong to one or the other of a small set of different spheres denoted by A_ν, B_ν, Γ_ν, etc.. This means that some of the spheres may be larger than the rest (as long as they do not overlap) or that they are characterized by a different (complex) dielectric function: $\epsilon_{\nu;A}\epsilon_0$, $\epsilon_{\nu;B}\epsilon_0$, etc., where ϵ_0 is the permittivity of vacuum. The spheres of a given plane occupy a fraction of the sites of a 2D space lattice, which is the same for all the planes of the slab and is given by

$$\mathbf{R}_n = n_1\mathbf{a}_1 + n_2\mathbf{a}_2 \tag{1}$$

where $\mathbf{a}_1$ and $\mathbf{a}_2$ are primitive vectors in the xy plane and $n_1, n_2 = 0, \pm 1, \pm 2, \pm 3, \ldots$. We note, however, that the fraction of the sites that are occupied by one or the other type of sphere may be different for different planes. The medium between the spheres in the slab is characterized by a real dielectric function $\epsilon(\omega)\epsilon_0$ and may be different from the

dielectric function of the medium on either side of the slab. The idea of the CPA is to replace each plane of spheres, by effective (frequency-dependent) scatterers occupying all the sites of the lattice given by Eq. (1); the scatterers of a given plane being the same, but possibly different from those of the other planes of the slab. As shown originally by Soven,[18] in relation to electron scattering by atomic centers, there is a way to obtain the effective scatterers so that, scattering by the effective periodic structure (periodic in the xy plane in our case) produces the best approximation to the given problem, that can be obtained by a corresponding periodic structure. Being a single-site approximation (**k**-independent effective scatterer), the method cannot deal with phenomena which are associated with large deviations from periodicity, but it can describe satisfactorily phenomena, such as those we shall be considering in this paper, which result from a relatively weak disorder.

Our main objective in this section is to obtain the equations that determine the above-mentioned effective scatterers. Once these have been determined, the calculation of the coefficients of transmission and absorption of light by the slab proceeds as in the case of periodic structures, which we know how to do.[9,11,23–25] In what follows we shall need, besides the space lattice of Eq. (1), the corresponding 2D reciprocal lattice defined by

$$\mathbf{g}=m_1\mathbf{b}_1+m_2\mathbf{b}_2, \tag{2}$$

where $m_1,m_2=0,\pm1,\pm2,\pm3,\ldots$ and $\mathbf{b}_1,\mathbf{b}_2$ are primitive vectors defined by

$$\mathbf{b}_i\cdot\mathbf{a}_j=2\pi\delta_{ij}, \quad i,j=1,2. \tag{3}$$

B. General formulas

We must now introduce a few formulas that we need for the development of the CPA method in relation to electromagnetic (EM) waves. We recall that a plane EM wave, of frequency ω and wave vector **q**, propagating in a homogeneous medium characterized by a real dielectric function $\epsilon(\omega)\epsilon_0$, has an electric-field component described by

$$\mathbf{E}(\mathbf{r},t)=Re[\mathbf{E}(\mathbf{r})\exp(-i\omega t)] \tag{4}$$

with

$$\mathbf{E}(\mathbf{r})=\mathbf{E}_0(\mathbf{q})\exp(i\mathbf{q}\cdot\mathbf{r}). \tag{5}$$

For our purposes it is convenient to write the component of the wave vector parallel to the plane of spheres as follows

$$\mathbf{q}_\parallel=\mathbf{k}_\parallel+\mathbf{g}', \tag{6}$$

where $\mathbf{k}_\parallel$ is the reduced wave vector of $\mathbf{q}_\parallel$ lying in the surface Brillouin zone (SBZ) corresponding to the reciprocal lattice of Eq. (2) and $\mathbf{g}'$ the appropriate reciprocal-lattice vector. Similarly, we write the wave vector of a plane wave of given frequency ω and a given component parallel to the plane of spheres, $\mathbf{q}_\parallel=\mathbf{k}_\parallel+\mathbf{g}$, as follows

$$\mathbf{K}_\mathbf{g}^\pm=(\mathbf{k}_\parallel+\mathbf{g},\pm[q^2-(\mathbf{k}_\parallel+\mathbf{g})^2]^{1/2}). \tag{7}$$

We assume throughout that the relative permeability of all constituent materials equals unity, so that $q=\sqrt{\epsilon}\omega/c$, where c denotes the velocity of light in vacuum. We need not write down explicitly the magnetic-field component of the EM wave.

$\mathbf{E}(\mathbf{r})$ is expanded in spherical waves as follows

$$\mathbf{E}(\mathbf{r})=\sum_{l=1}^{\infty}\sum_{m=-l}^{l}\left[\frac{i}{q}\,a_{lm}^{0E}\nabla\times j_l(qr)\mathbf{X}_{lm}(\hat{\mathbf{r}})+a_{lm}^{0H}j_l(qr)\mathbf{X}_{lm}(\hat{\mathbf{r}})\right] \tag{8}$$

where $\mathbf{X}_{lm}(\hat{\mathbf{r}})$ are the usual vector spherical harmonics, $\hat{\mathbf{r}}$ denotes the angular variables of $\mathbf{r}$, and $j_l(qr)$ is the spherical Bessel function. The coefficients a_{lm}^{0P}, where $P=E,H$, are written as

$$a_{lm}^{0P}=\sum_i A_{lm;i}^{0P}(\mathbf{q})\;E_{0;i}(\mathbf{q}), \tag{9}$$

where $i=x,y,z$. Explicit relations for the coefficients $A_{lm;i}^{0P}$ are to be found in Ref. 23. In general, when a wave is incident on a sphere, centered at the origin of coordinates, there results a scattered wave given by

$$\mathbf{E}^{sc}(\mathbf{r})=\sum_{l=1}^{\infty}\sum_{m=-l}^{l}\left[\frac{i}{q}\,a_{lm}^{+E}\nabla\times h_l^+(qr)\mathbf{X}_{lm}(\hat{\mathbf{r}})+a_{lm}^{+H}h_l^+(qr)\mathbf{X}_{lm}(\hat{\mathbf{r}})\right], \tag{10}$$

where $h_l^+(qr)$ is the spherical Hankel function. The total wavefield outside the sphere is the sum of the fields given by Eqs. (8) and (10). The coefficients a_{lm}^{+P} of the scattered field are related to those of the incident wave through the scattering matrix $\mathbf{T}(\omega)$. We have

$$\boldsymbol{a}^+=\mathbf{T}\boldsymbol{a}^0. \tag{11}$$

Here and throughout the paper, a matrix notation in the representation lmP is implied. In the case of an ordinary spherical scatterer, the **T** matrix is diagonal: $T_{lm;l'm'}^{PP'}=T_{lm}^P\delta_{ll'}\delta_{mm'}\delta_{PP'}$ but, the CPA effective scattering matrix, to be introduced in what follows, turns out to be nondiagonal even for spherical scatterers.

C. The CPA equations

We assume, to begin with, that the νth plane of spheres (the nonperiodic array of different spheres described in Sec. II A) can be described, in the spirit of the CPA method, by a periodic array of same spheres centered on the lattice sites given by Eq. (1); each sphere is represented by an effective matrix $\langle\mathbf{T}\rangle_\nu$ to be determined. When the plane wave of Eq. (4) is incident on this plane of spheres, the wave scattered from the central sphere (at $n_1=n_2=0$) is given by

$$\mathbf{b}^+=\langle\mathbf{T}\rangle_\nu\mathbf{b}^0 \tag{12}$$

$$\mathbf{b}^0=(\boldsymbol{a}^0+\mathbf{b}'), \tag{13}$$

where $\mathbf{b}^0$ stands for the total wave incident on the central sphere; $\boldsymbol{a}^0$ represents the incident plane wave and $\mathbf{b}'$ takes

into account the wave incident on the central sphere, which is due to the waves scattered from all the other spheres of the plane. We know that[23,24]

$$\mathbf{b}' = \mathbf{\Omega}\mathbf{b}^{+}. \tag{14}$$

The matrix elements of $\mathbf{\Omega}$ depend on the geometry of the plane, on the reduced wave vector $\mathbf{k}_{\parallel}$ and on the frequency ω of the incident wave. They depend also on the dielectric function of the medium surrounding the spheres, but they do not depend on the scattering properties of the individual spheres. We need not give here the explicit expressions for the matrix elements of $\mathbf{\Omega}$, which can be found in Refs. 23 and 24. By combining Eqs. (12), (13), and (14) one obtains

$$\boldsymbol{b}^0 = [\mathbf{I} - \mathbf{\Omega}\langle \mathbf{T}\rangle_\nu]^{-1}\boldsymbol{a}^0. \tag{15}$$

When the plane of spheres under consideration is one of the planes of a slab, $\boldsymbol{a}^0$ includes besides the externally incident light, that which is due to the waves scattered by the other planes of the slab.

Let us now replace the scatterer $\langle \mathbf{T}\rangle_\nu$ at the central sphere of the νth plane by an actual scatterer $\mathbf{T}_{\nu;\alpha}$ ($\alpha = A_\nu, B_\nu, \Gamma_\nu, \ldots$). Then the scattered wave from this sphere consists of the term given by Eq. (12) and, to begin with, an additional term given by

$$\Delta\mathbf{T}_{\nu;\alpha}\mathbf{b}^0, \tag{16}$$

where

$$\Delta\mathbf{T}_{\nu;\alpha} \equiv \mathbf{T}_{\nu;\alpha} - \langle \mathbf{T}\rangle_\nu. \tag{17}$$

The wave obtained from Eq. (16) will be multiply scattered by *all the spheres in the slab*, including the central sphere of the νth plane (represented by $\langle \mathbf{T}\rangle_\nu$), producing a further contribution to the incident on this sphere wave, which may be written as follows

$$\tilde{\mathbf{G}}_\nu^{00}\Delta\mathbf{T}_{\nu;\alpha}\mathbf{b}^0, \tag{18}$$

where $\tilde{\mathbf{G}}_\nu^{00}$ represents the contribution of all possible paths by which a wave outgoing from the central sphere of the νth plane [represented by a set of coefficients in the way that the wave described by Eq. (10) is represented by the coefficients a_{lm}^{+P}] produces an incident wave on the same sphere [represented by a set of coefficients in the way that the wave described by Eq. (8) is represented by the coefficients a_{lm}^{0P}], after scattering in all possible ways (sequences) by the scatterers $\langle \mathbf{T}\rangle_\lambda$, $\lambda = 1, \ldots, N$, at all sites of the N planes. Because of Eq. (18), there will be a further contribution to the scattered wave from the central sphere of the νth plane given by

$$\Delta\mathbf{T}_{\nu;\alpha}\tilde{\mathbf{G}}_\nu^{00}\Delta\mathbf{T}_{\nu;\alpha}\mathbf{b}^0. \tag{19}$$

The same process is repeated infinitely many times and this leads to the following expression for the scattered wave from the central sphere of the νth plane due to $\Delta\mathbf{T}_{\nu;\alpha}$

$$\begin{aligned}(\mathbf{I} + \Delta\mathbf{T}_{\nu;\alpha}\tilde{\mathbf{G}}_\nu^{00} + \Delta\mathbf{T}_{\nu;\alpha}\tilde{\mathbf{G}}_\nu^{00}\Delta\mathbf{T}_{\nu;\alpha}\tilde{\mathbf{G}}_\nu^{00} + \cdots)\Delta\mathbf{T}_{\nu;\alpha}\mathbf{b}^0 \\ = (\mathbf{I} - \Delta\mathbf{T}_{\nu;\alpha}\tilde{\mathbf{G}}_\nu^{00})^{-1}\Delta\mathbf{T}_{\nu;\alpha}\mathbf{b}^0, \quad \text{for} \quad \nu = 1,2,\ldots,N.\end{aligned} \tag{20}$$

The effective CPA matrices $\langle \mathbf{T}\rangle_\nu$, $\nu = 1,2,\ldots,N$, are obtained, in the manner originally proposed by Soven,[18] by demanding that the scattered wave of Eq. (20) vanishes on averaging, i.e., we demand that

$$\sum_\alpha C_{\nu;\alpha}(\mathbf{I} - \Delta\mathbf{T}_{\nu;\alpha}\tilde{\mathbf{G}}_\nu^{00})^{-1}\Delta\mathbf{T}_{\nu;\alpha} = 0, \quad \nu = 1,2,\ldots,N, \tag{21}$$

where $C_{\nu;\alpha}$ denotes the concentration of the scatterer $\alpha = A_\nu, B_\nu, \Gamma_\nu$, etc. of the νth plane. Obviously,

$$\sum_\alpha C_{\nu;\alpha} = 1. \tag{22}$$

Equation (21) determines uniquely the effective matrices $\langle \mathbf{T}\rangle_\nu$, $\nu = 1,2,\ldots,N$, which appear in the propagators $\tilde{\mathbf{G}}_\nu^{00}$ (see below). We note that Eq. (21) is the extension of the CPA condition, derived earlier, for a single plane of scatterers [see Eq. (12) of Ref. 15]. In order to proceed further, we need an explicit expression for $\tilde{\mathbf{G}}_\nu^{00}$. One can see that this operator can be written as a sum of three terms as follows

$$\tilde{\mathbf{G}}_\nu^{00} = \tilde{\mathbf{D}}_\nu^{00} + \sum_n \tilde{\mathbf{P}}_\nu^{0n}\langle \mathbf{T}\rangle_\nu \tilde{\mathbf{D}}_\nu^{n0} + \tilde{\mathbf{P}}_\nu^{00}. \tag{23}$$

The matrix $\tilde{\mathbf{D}}_\nu^{nm}$ represents all the possible scattering paths *within* the νth plane by which a wave outgoing from the mth sphere of this plane produces an incident wave on the nth sphere of the same plane, after scattering in all possible ways by all the spheres of this plane including the central sphere (every sphere represented by $\langle \mathbf{T}\rangle_\nu$). $\tilde{\mathbf{D}}_\nu^{nm}$ has been discussed in Ref. 15 and we need not repeat the arguments here. We have

$$\tilde{\mathbf{D}}_\nu^{nm}(\omega) = \frac{1}{S_0}\int\int_{SBZ} d^2k_{\parallel}\exp(i\mathbf{k}_{\parallel}\cdot\mathbf{R}_{nm})\mathbf{D}_\nu(\mathbf{k}_{\parallel};\omega) \tag{24}$$

$$\mathbf{D}_\nu(\mathbf{k}_{\parallel};\omega) = [\mathbf{I} - \mathbf{\Omega}(\mathbf{k}_{\parallel};\omega)\langle \mathbf{T}(\omega)\rangle_\nu]^{-1}\mathbf{\Omega}(\mathbf{k}_{\parallel};\omega), \tag{25}$$

where $\mathbf{R}_{nm} = \mathbf{R}_n - \mathbf{R}_m$, S_0 is the area of the SBZ corresponding to Eq. (2), and $\mathbf{\Omega}(\mathbf{k}_{\parallel};\omega)$ is the matrix introduced by Eq. (14).

The matrix $\tilde{\mathbf{P}}_\nu^{0n}$ appearing in the second and third terms of Eq. (23) represents all scattering paths by which an outgoing wave from the nth sphere of the νth plane *exits* from that plane to produce an incident wave on the central sphere of the same plane after scattering in all possible ways by all the planes of spheres of the slab, including the νth plane. In the next section we show how to calculate $\tilde{\mathbf{P}}_\nu^{0n}$ and $\tilde{\mathbf{G}}_\nu^{00}$.

D. Calculation of $\tilde{\mathbf{P}}_\nu^{0n}$ and $\tilde{\mathbf{G}}_\nu^{00}$

A wave outgoing from the nth sphere of the νth plane has the form

$$\begin{aligned}\mathbf{E}^{sc}(\mathbf{r}) = \sum_{l=1}^{\infty}\sum_{m=-l}^{l}\Bigg[\frac{i}{q}\, b_{lm}^{+E}(n;\nu)\boldsymbol{\nabla}\times h_l^{+}(qr_{n\nu})\mathbf{X}_{lm}(\hat{\mathbf{r}}_{n\nu}) \\ + b_{lm}^{+H}(n;\nu)h_l^{+}(qr_{n\nu})\mathbf{X}_{lm}(\hat{\mathbf{r}}_{n\nu})\Bigg],\end{aligned} \tag{26}$$

where $\mathbf{r}_{n\nu}$ is the position vector with respect to the center (at $\mathbf{R}_n$) of the nth sphere of the νth plane. Using the following identities

$$h_l^+(qr_{n\nu})\mathbf{X}_{lm}(\hat{\mathbf{r}}_{n\nu}) = \frac{1}{S_0}\int\int_{SBZ} d^2k_\parallel \sum_{\mathbf{g}} \boldsymbol{\Delta}^H_{lm}(\mathbf{K}_\mathbf{g}^\pm)\exp(\mathrm{i}\mathbf{K}_\mathbf{g}^\pm\cdot\mathbf{r}_{n\nu}) \tag{27}$$

$$\frac{i}{q}\boldsymbol{\nabla}\times h_l^+(qr_{n\nu})\mathbf{X}_{lm}(\hat{\mathbf{r}}_{n\nu}) = \frac{1}{S_0}\int\int_{SBZ} d^2k_\parallel \sum_{\mathbf{g}} \boldsymbol{\Delta}^E_{lm}(\mathbf{K}_\mathbf{g}^\pm)\exp(\mathrm{i}\mathbf{K}_\mathbf{g}^\pm\cdot\mathbf{r}_{n\nu}) \tag{28}$$

with

$$\boldsymbol{\Delta}^H_{lm}(\mathbf{K}_\mathbf{g}^\pm) = \frac{2\pi(-\mathrm{i})^l}{qA_0K^+_{\mathbf{g}z}}\mathbf{X}_{lm}(\hat{\mathbf{K}}_\mathbf{g}^\pm) \tag{29}$$

$$\boldsymbol{\Delta}^E_{lm}(\mathbf{K}_\mathbf{g}^\pm) = -\frac{\mathbf{K}_\mathbf{g}^\pm}{q}\times\boldsymbol{\Delta}^H_{lm}(\mathbf{K}_\mathbf{g}^\pm),$$

where A_0 is the area of the unit cell of the space lattice given by Eq. (1), we can expand the wave of Eq. (26) into a sum of plane waves propagating or decaying away from the νth plane as follows. To the right of the νth plane we have

$$\mathbf{E}^{out\ +}(\mathbf{r}) = \frac{1}{S_0}\int\int_{SBZ} d^2k_\parallel \sum_{\mathbf{g}} \mathbf{E}_\mathbf{g}^{out\ +}(\mathbf{k}_\parallel) \times\exp\{\mathrm{i}\mathbf{K}_\mathbf{g}^+\cdot[\mathbf{r}-\mathbf{A}_r(\nu)]\} \tag{30}$$

with

$$E^{out\ +}_{\mathbf{g};i}(\mathbf{k}_\parallel) = \exp\{-\mathrm{i}[\mathbf{k}_\parallel\cdot\mathbf{R}_n-\mathbf{K}_\mathbf{g}^+\cdot\mathbf{d}_r(\nu)]\} \times\sum_{l=1}^{\infty}\sum_{m=-l}^{l}\sum_{P=E,H}\Delta^P_{lm;i}(\mathbf{K}_\mathbf{g}^+)b^{+P}_{lm}(n;\nu), \tag{31}$$

where $i=x,y,z$ and $\mathbf{A}_r(\nu)$ is a reference point on the right of the νth plane at $\mathbf{d}_r(\nu)$ from its center (see Fig. 1). To the left of the νth plane we have

$$\mathbf{E}^{out\ -}(\mathbf{r}) = \frac{1}{S_0}\int\int_{SBZ} d^2k_\parallel \sum_{\mathbf{g}} \mathbf{E}_\mathbf{g}^{out\ -}(\mathbf{k}_\parallel) \times\exp\{\mathrm{i}\mathbf{K}_\mathbf{g}^-\cdot[\mathbf{r}-\mathbf{A}_l(\nu)]\} \tag{32}$$

with

$$E^{out\ -}_{\mathbf{g};i}(\mathbf{k}_\parallel) = \exp\{-\mathrm{i}[\mathbf{k}_\parallel\cdot\mathbf{R}_n+\mathbf{K}_\mathbf{g}^-\cdot\mathbf{d}_l(\nu)]\} \times\sum_{l=1}^{\infty}\sum_{m=-l}^{l}\sum_{P=E,H}\Delta^P_{lm;i}(\mathbf{K}_\mathbf{g}^-)b^{+P}_{lm}(n;\nu), \tag{33}$$

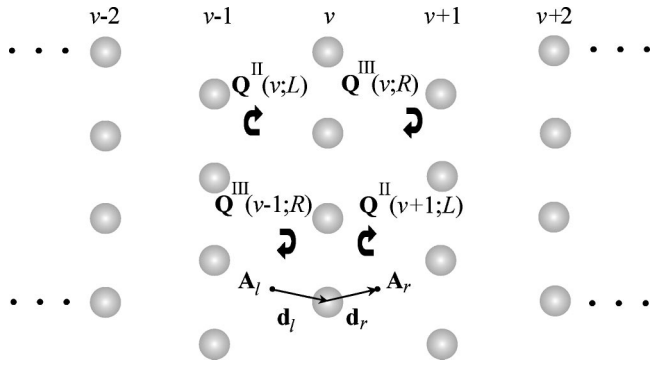

FIG. 1. The $\mathbf{Q}$ matrices appearing in Eq. (42). The position vectors $\mathbf{d}_l$, $\mathbf{d}_r$ of the νth layer along with the corresponding origins $\mathbf{A}_l$, $\mathbf{A}_r$ are also shown.

where $\mathbf{A}_l(\nu)$ is a reference point to the left of the νth plane at $-\mathbf{d}_l(\nu)$ from its center (see Fig. 1). The plane waves of Eq. (30) will be multiply reflected between two parts of the slab, the first (right part) consisting of all planes to the right of the νth plane, and the second (left part) consisting of all planes to the left of the $(\nu+1)$th plane (including the νth plane), to produce a set of plane waves incident on the νth plane from the right, which we can write formally as follows

$$\mathbf{E}^{in\ -}(\mathbf{r}) = \frac{1}{S_0}\int\int_{SBZ} d^2k_\parallel \sum_{\mathbf{g}} \mathbf{E}_\mathbf{g}^{in\ -}(\mathbf{k}_\parallel) \times\exp\{\mathrm{i}\mathbf{K}_\mathbf{g}^-\cdot[\mathbf{r}-\mathbf{A}_r(\nu)]\} \tag{34}$$

with

$$E^{in\ -}_{\mathbf{g};i}(\mathbf{k}_\parallel) = \sum_{\mathbf{g}',i'}\{\mathbf{Q}^{\mathrm{III}}(\nu;R)[\mathbf{I}-\mathbf{Q}^{\mathrm{II}}(\nu+1;L) \times\mathbf{Q}^{\mathrm{III}}(\nu;R)]^{-1}\}_{\mathbf{g}i;\mathbf{g}'i'}E^{out\ +}_{\mathbf{g}';i'}(\mathbf{k}_\parallel), \tag{35}$$

where $\mathbf{Q}^{\mathrm{II}}(\nu+1;L)$ and $\mathbf{Q}^{\mathrm{III}}(\nu;R)$ are the appropriate matrices that determine the reflection (diffraction) of a plane wave [defined by Eq. (7)] by the left and the right parts of the slab respectively, as defined above. These matrices are shown schematically in Fig. 1.

Similarly, the plane waves of Eq. (32) will be multiply reflected between two parts of the slab, the first (left part) consisting of all planes to the left of the νth plane and the second (right part) consisting of all planes to the right of the $(\nu-1)$th plane (including the νth plane), to produce a set of plane waves incident on the νth plane from the left, which we can write formally as follows

$$\mathbf{E}^{in\ +}(\mathbf{r}) = \frac{1}{S_0}\int\int_{SBZ} d^2k_\parallel \sum_{\mathbf{g}} \mathbf{E}_\mathbf{g}^{in\ +}(\mathbf{k}_\parallel) \times\exp\{\mathrm{i}\mathbf{K}_\mathbf{g}^+\cdot[\mathbf{r}-\mathbf{A}_l(\nu)]\} \tag{36}$$

with

$$E^{in\ +}_{\mathbf{g};i}(\mathbf{k}_\parallel) = \sum_{\mathbf{g}',i'}\{\mathbf{Q}^{\mathrm{II}}(\nu;L)[\mathbf{I}-\mathbf{Q}^{\mathrm{III}}(\nu-1;R) \times\mathbf{Q}^{\mathrm{II}}(\nu;L)]^{-1}\}_{\mathbf{g}i;\mathbf{g}'i'}E^{out\ -}_{\mathbf{g}';i'}(\mathbf{k}_\parallel) \tag{37}$$

where $\mathbf{Q}^{\mathrm{II}}(\nu;L)$ and $\mathbf{Q}^{\mathrm{III}}(\nu-1;R)$ are again the appropriate matrices, shown schematically in Fig. 1. A more detailed description of these matrices and the way these are calculated is to be found in section 2.4 of Ref. 23. We note that for $\nu=1(N)$ we have only waves incident from the right (left).

Each plane wave in Eqs. (34) and (36) can be expanded in spherical waves about the central sphere of the νth plane using Eq. (9). For a plane wave $\mathbf{E}_{\mathbf{g}}^{in\ -}(\mathbf{k}_\parallel)\exp\{\mathrm{i}\mathbf{K}_{\mathbf{g}}^{-}\cdot[\mathbf{r}-\mathbf{A}_r(\nu)]\}$, incident on the νth plane from the right, the coefficients in Eq. (9) are given by

$$a_{lm}^{0P}(\mathbf{K}_{\mathbf{g}}^{-})=\exp[-\mathrm{i}\mathbf{K}_{\mathbf{g}}^{-}\cdot\mathbf{d}_r(\nu)]\sum_i A_{lm;i}^{0P}(\mathbf{K}_{\mathbf{g}}^{-})E_{\mathbf{g};i}^{in\ -}(\mathbf{k}_\parallel). \tag{38}$$

And for a plane wave, $\mathbf{E}_{\mathbf{g}}^{in\ +}(\mathbf{k}_\parallel)\exp\{\mathrm{i}\mathbf{K}_{\mathbf{g}}^{+}\cdot[\mathbf{r}-\mathbf{A}_l(\nu)]\}$, incident on the νth plane from the left, the coefficients in Eq. (9) are

$$a_{lm}^{0P}(\mathbf{K}_{\mathbf{g}}^{+})=\exp[\mathrm{i}\mathbf{K}_{\mathbf{g}}^{+}\cdot\mathbf{d}_l(\nu)]\sum_i A_{lm;i}^{0P}(\mathbf{K}_{\mathbf{g}}^{+})E_{\mathbf{g};i}^{in\ +}(\mathbf{k}_\parallel). \tag{39}$$

Finally, to obtain the wave incident on the central sphere of the νth plane, which derives from the outgoing wave of Eq. (26), we must add to the waves given by Eqs. (34) and (36) that which is due to the wave scattered from all the other spheres of the νth plane. The expansion in terms of spherical waves about the central sphere of the νth plane of the sum of all these waves has coefficients that are given, in accordance with Eq. (15), by

$$\tilde{\mathbf{P}}_\nu^{0n}\boldsymbol{b}^{+}(n;\nu)=\frac{1}{S_0}\int\int_{SBZ}\sum_{\mathbf{g}}\sum_{s=\pm}[\mathbf{I}-\boldsymbol{\Omega}\langle\mathbf{T}\rangle_\nu]^{-1}\boldsymbol{a}^{0}(\mathbf{K}_{\mathbf{g}}^{s}) \tag{40}$$

$$=\left\{\frac{1}{S_0}\int\int_{SBZ}d^2k_\parallel\exp(-\mathrm{i}\mathbf{k}_\parallel\cdot\mathbf{R}_n)\times[\mathbf{I}-\boldsymbol{\Omega}\langle\mathbf{T}\rangle_\nu]^{-1}\boldsymbol{\Gamma}_{\boldsymbol{\nu}}\right\}\boldsymbol{b}^{+}(n;\nu), \tag{41}$$

where $\boldsymbol{\Gamma}_\nu(\mathbf{k}_\parallel;\omega)$ is a matrix defined by

$$\Gamma_{lm;l'm';\nu}^{PP'}(\mathbf{k}_\parallel;\omega)=\sum_{\mathbf{g},i}\sum_{\mathbf{g}',i'}\{\exp[-\mathrm{i}(\mathbf{K}_{\mathbf{g}}^{-}-\mathbf{K}_{\mathbf{g}'}^{+})\cdot\mathbf{d}_r(\nu)]A_{lm;i}^{0P}(\mathbf{K}_{\mathbf{g}}^{-})\times[\mathbf{Q}^{\mathrm{III}}(\nu;R)[\mathbf{I}-\mathbf{Q}^{\mathrm{II}}(\nu+1;L)\mathbf{Q}^{\mathrm{III}}(\nu;R)]^{-1}]_{\mathbf{g}i;\mathbf{g}'i'}\Delta_{l'm';i'}^{P'}(\mathbf{K}_{\mathbf{g}'}^{+})+\exp[\mathrm{i}(\mathbf{K}_{\mathbf{g}}^{+}-\mathbf{K}_{\mathbf{g}'}^{-})\cdot\mathbf{d}_l(\nu)]A_{lm;i}^{0P}(\mathbf{K}_{\mathbf{g}}^{+})\times[\mathbf{Q}^{\mathrm{II}}(\nu;L)[\mathbf{I}-\mathbf{Q}^{\mathrm{III}}(\nu-1;R)\mathbf{Q}^{\mathrm{II}}(\nu;L)]^{-1}]_{\mathbf{g}i;\mathbf{g}'i'}\Delta_{l'm';i'}^{P'}(\mathbf{K}_{\mathbf{g}'}^{-})\}. \tag{42}$$

Therefore, $\tilde{\mathbf{P}}_\nu^{0n}$ is given by the term in the braces of Eq. (41). Accordingly the second term in Eq. (23) becomes

$$\sum_n \tilde{\mathbf{P}}_\nu^{0n}\langle\mathbf{T}\rangle_\nu\ \tilde{\mathbf{D}}_\nu^{n0}=\frac{1}{S_0}\int\int_{SBZ}d^2k_\parallel\{[\mathbf{I}-\boldsymbol{\Omega}\langle\mathbf{T}\rangle_\nu]^{-1}\boldsymbol{\Gamma}_\nu\langle\mathbf{T}\rangle_\nu\mathbf{D}_\nu\}, \tag{43}$$

where $\mathbf{D}_\nu(\mathbf{k}_\parallel;\omega)$ is given by Eq. (25). To derive Eq. (43) we substitute on the left of this equation $\tilde{\mathbf{D}}_\nu^{n0}(\omega)$ according to Eq. (24) and use the relation

$$\frac{1}{S_0}\sum_n \exp[\mathrm{i}(\mathbf{k}_\parallel-\mathbf{k}_\parallel')\cdot\mathbf{R}_n]=\delta(\mathbf{k}_\parallel-\mathbf{k}_\parallel'). \tag{44}$$

Finally, the matrix $\tilde{\mathbf{G}}_\nu^{00}$, defined by Eq. (23), is given by

$$\tilde{\mathbf{G}}_\nu^{00}=\frac{1}{S_0}\int\int_{SBZ}d^2k_\parallel\{[\mathbf{I}-\boldsymbol{\Omega}\langle\mathbf{T}\rangle_\nu]^{-1}[\boldsymbol{\Omega}+\boldsymbol{\Gamma}_\nu(\mathbf{I}+\langle\mathbf{T}\rangle_\nu\times[\mathbf{I}-\boldsymbol{\Omega}\langle\mathbf{T}\rangle_\nu]^{-1}\boldsymbol{\Omega})]\}. \tag{45}$$

III. NUMERICAL COMPUTATION OF $\langle\mathbf{T}\rangle_\nu$

The solution of Eqs. (21) to obtain the effective matrices $\langle\mathbf{T}\rangle_\nu$, $\nu=1,2,\ldots,N$, in the general case when a large number of scatterers ($\alpha=A_\nu$, B_ν, Γ_ν, . . .) are present in the different planes of the slab, is computationally time consuming. The simplest case arises when the lattice sites of Eq. (1) of the νth plane are occupied by one or the other of two scatterers: A_ν or B_ν. One can show that in this case Eqs. (21) become

$$\langle\mathbf{T}\rangle_\nu=C_{\nu;A}\mathbf{T}_{\nu;A}+C_{\nu;B}\mathbf{T}_{\nu;B}-\Delta\mathbf{T}_{\nu;A}\tilde{\mathbf{G}}_\nu^{00}\Delta\mathbf{T}_{\nu;B} \tag{46}$$

with $\nu=1,2,\ldots,N$. And we remember that $\tilde{\mathbf{G}}_\nu^{00}$ depends on all $\langle\mathbf{T}\rangle_\nu$ matrices.

We solve the above equations iteratively, as follows: we begin with a reasonable initial input for $\langle\mathbf{T}\rangle_\nu$, e.g., the average $\mathbf{T}$-matrix approximation[26] (ATA): $C_{\nu;A}\mathbf{T}_{\nu;A}+C_{\nu;B}\mathbf{T}_{\nu;B}$ on the r.h.s. of Eq. (46), to obtain a first approximation to $\langle\mathbf{T}\rangle_\nu$. The same procedure is repeated a number of times, using as input at each iteration step a proper mixture of the output matrices $\langle\mathbf{T}\rangle_\nu$ of previous iterations, until convergence is obtained. In order to accelerate the rate of convergence of the iterative procedure we have made use of a special iteration scheme, the generalized Anderson method.[27] The number of iterations needed to achieve convergence depends on the frequency ω of the light for which the calcula-

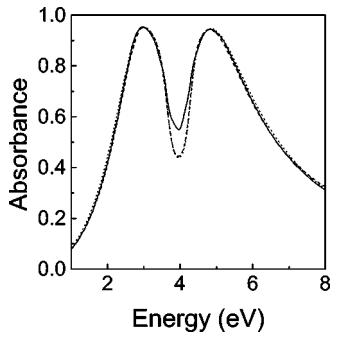

FIG. 2. Absorbance of light incident normally on a slab of an fcc crystal consisting of plasma spheres ($S=50$ Å , $\hbar\omega_p=9.2$ eV, $\hbar\tau^{-1}=0.2$ eV) embedded in gelatine ($\epsilon=2.37$) and occupying randomly 75% of the lattice sites. The slab consists of 129 planes parallel to the (001) surface of fcc and the volume fraction occupied by the spheres is $f=0.1$. The CPA (ATA) results are denoted by the solid (dashed) line. The dotted line refers to the corresponding ordered system of the same volume fraction *f*.

tion is done. On the average, 300 iterations gave good convergence (an accuracy of 10^{-6}) for the cases examined in Sec. IV. The angular momentum space is truncated by introducing an angular momentum cut-off number l_{max}. Similarly, we limit the number of reciprocal-lattice vectors to be included in the calculation, to the g_{max} vectors with magnitude less than a certain number. For the cases considered in Sec. IV we obtain an accurate description of the EM field (and of the relevant matrices in the spherical and plane-wave representations) by putting $l_{max}=4$ and $g_{max}=13$.

The evaluation of $\tilde{\mathbf{G}}_{\nu}^{00}$ requires a numerical integration over the entire SBZ [see Eq. (45)]. Using symmetry to reduce the area of integration to a part of SBZ is not profitable in the present case. However, when one deals with light-absorbing spheres (described by a complex dielectric function), as in the case under consideration in Sec. IV, the intergrand in Eq. (45) is a relatively smooth function of $\mathbf{k}_{\parallel}$, and the integration can be performed without much difficulty by subdividing the SBZ (a square in our examples) into small squares, within which a nine-point integration formula[28] is very efficient. We have also tried other integration techniques based on sets of special points with corresponding weights,[29,30] but, in our case, the nine-point integration formula proved the more efficient. Using this formula we managed good convergence with a total of 81 points in the SBZ. We note, however, that in a case involving nonabsorbing spheres (described by a real dielectric function) the

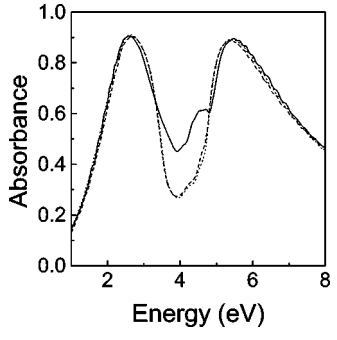

FIG. 3. The same as in Fig. 2, except that $f=0.2$.

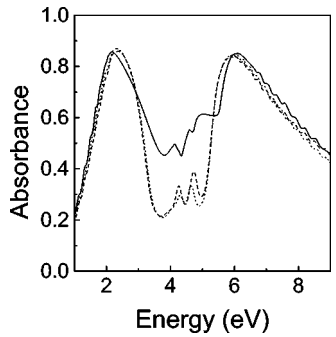

FIG. 4. The same as in Fig. 2, except that $f=0.3$.

intergrand in Eq. (45) may not be varying smoothly and other means[31] would be necessary for the evaluation of the $\mathbf{k}_{\parallel}$ integration. We hope to deal with this problem, in relation to non-absorbing photonic crystals, in another article.

Once the effective matrices $\langle\mathbf{T}\rangle_{\nu}$, $\nu=1,2,\ldots,N$, have been determined, and put in place at the lattice sites defined by Eq. (1) of the corresponding *N* planes that make up the slab, the calculation of the reflection transmission, and absorption coefficients of light incident on the slab can be calculated in the manner described in Ref. 23. We need not say anything more here.

IV. RESULTS AND DISCUSSION

We used the method described in the previous sections to calculate the absorbance of a slab consisting of nonoverlapping metallic spheres occupying randomly the sites of an fcc lattice viewed as a succession of (001) planes. We considered a relatively thick slab consisting of 129 layers (planes of spheres), which allows us to disregard end effects: we assume that the effective matrix $\langle\mathbf{T}\rangle$ is the same for every layer and the same with that obtained for a layer of an infinitely thick slab. We have further assumed that the individual metallic sphere is a plasma sphere, described by a Drude dielectric function

$$\epsilon_S(\omega)=1-\frac{\omega_p^2}{\omega(\omega+i\tau^{-1})}, \tag{47}$$

where ω_p stands for the bulk plasma frequency of the metal and τ is the relaxation time of the conduction band electrons. We compare the absorbance of the above disordered slab with that of a slab of perfect periodicity containing the same total mass of plasma spheres, so that the fractional volume *f* occupied by the spheres is the same in both cases. This means that the lattice constant of the fcc lattice for the ordered slab [$a_{ord}=S(16\pi/3f)^{1/3}$, where *S* is the radius of the spheres] is larger than that of the disordered slab [$a=S(16\pi C/3f)^{1/3}$, where *C* is the concentration of the spheres]. We remember that for an fcc lattice (fully occupied) of touching spheres $f=0.74$. In every case the spheres are embedded in a dielectric medium ($\epsilon=2.37$, corresponding to gelatine), and we assume that the same medium extends in all space to the left and right of the slab.

The results shown in Figs. 2–4 were obtained for light incident normally on a slab consisting of plasma spheres occupying 75% of an fcc lattice. In every case the spheres are all the same, with a radius $S=50$ Å, and we have as-

sumed, following Ref. 32, a resonance energy $\hbar\omega_p = 9.2$ eV and $\hbar\tau^{-1} = 0.2$ eV. The volume fraction occupied by the spheres is: $f = 0.1$ (corresponding to a lattice constant $a = 250.44$ Å) in Fig. 2; $f = 0.2$ ($a = 198.78$ Å) in Fig. 3, and $f = 0.3$ ($a = 173.65$ Å) in Fig. 4. The absorbance of the disordered slab calculated in the manner we have described (CPA method) is shown by a solid line; the absorbance of the corresponding ordered slab is shown by the dotted line; the broken line is obtained using the so-called average **T**-matrix approximation (ATA), according to which the randomly occupied lattice is replaced by one fully occupied by spheres each of which is characterized by an effective scattering matrix

$$\langle \mathbf{T} \rangle_{ATA} = C\mathbf{T}, \tag{48}$$

where C denotes the concentration of the spheres and **T** the scattering matrix of the actual spheres. We see that the results for the disordered slab obtained by the ATA are practically identical with those of the corresponding ordered slab. We can understand why the ATA results coincide with those of the ordered structure, at least in the electrostatic limit, by using the Maxwell Garnett (MG) equation

$$\frac{\bar{\epsilon} - \epsilon}{\bar{\epsilon} + 2\epsilon} = \frac{4}{3}\pi n \alpha \tag{49}$$

where $n = 3f/4\pi S^3$; $\bar{\epsilon}$ is the dielectric function of the effective medium, ϵ is that of the host medium and α is the polarizability of a single sphere in the host medium given by

$$\alpha(\omega) = S^3 \frac{\epsilon_S(\omega) - \epsilon}{\epsilon_S(\omega) + 2\epsilon}. \tag{50}$$

The ATA, in the electrostatic limit, replaces the random distribution of the partly empty lattice by a lattice fully occupied by same spheres with polarizability $C\alpha(\omega)$, where C is the concentration of the spheres, and applies to the latter the MG formula [Eq. (49)]. However, multiplying the polarizability $\alpha(\omega)$ by C is equivalent to multiplying the volume of the spheres by C [see Eq. (50)], which tells us that the r.h.s. of Eq. (49) and, therefore $\bar{\epsilon}$, does not change in this approximation.

The CPA gives nearly the same results for the disordered as those obtained for the ordered slab for $f = 0.1$, but as f increases differences between the two do appear. The main difference relates to the dip between the two peaks in the absorbance curve which is due to a frequency gap of the EM field in the corresponding infinite crystal (a slab extending from $z = -\infty$ to $z = +\infty$). The physical origin of this gap which is moderated by the presence of absorption is discussed in Ref. 32; it is shown there that this gap is the result of hybridization between a narrow band of interacting dipole resonances centered on the spheres and a wide band of freely propagating waves in an effective host medium. Evidently disorder reduces further the effect of the above-mentioned frequency gap on the absorbance curve. The structure (peaks) in the absorbance curve in the region of the dip, derives mainly from higher-multipole ($l > 1$) bands, in the manner explained in Ref. 32. Again, it does appear that disorder amplifies the effect of these higher-multipole resonances. Some structure may also arise from the removal of

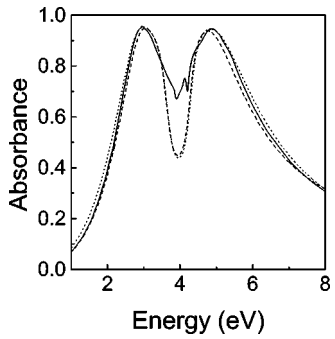

FIG. 5. Absorbance of light incident normally on a slab consisting of plasma spheres [the same as in Fig. (2)] occupying 50% of the sites of an fcc lattice; $f = 0.1$ ($a = 154.71$ Å).

the degeneracy between dipolar terms of different m (see below). The ripples appearing in the low- and high-frequency tails of the absorbance curve are due to the finite size of the slab, which gives rise to Fabry-Perot type oscillations.

One observes, also, with increasing f, a slight shift of the lower-frequency peak to lower frequencies, and a corresponding small shift of the high-frequency peak to higher frequencies. But we do not find a dramatic shift in either of these peaks, in contrast to what might be expected from the work of Liebsch and Persson.[22] In order to further clarify this point, we calculated the absorbance of a slab consisting of plasma spheres (the same as in Figs. 2–4) occupying randomly 50% (instead of 75%) of the sites of an fcc lattice (the same lattice as in Fig. 2, except that in the present case the lattice constant is changed to $a = 154.71$ Å , so that $f = 0.1$ as in Fig. 2). The results, shown in Fig. 5, again show no dramatic difference between the ordered and disordered slabs except in one respect: there appears an additional peak in the absorbance curve in the region of the dip of the curve. In contrast to the peaks in the dips of the curves of Figs. 3 and 4, which mirror multipole peaks of the ordered case, the peak in question is dipolar in origin. In order to clarify this point we calculated the absorbance of a single CPA scatterer. The energy absorbed per unit time by a scatterer of spherical shape is given by the negative integral of the Poynting vector over the surface of the sphere. We denote the average of this quantity over a period $T = 2\pi/\omega$ by $\bar{w}$. Using the multipole expansions (8) and (10) of the EM field we obtain

$$\bar{w} = -\frac{c^3 \epsilon_0}{2\omega^2 \sqrt{\epsilon}} Re \sum_{l=1}^{\infty} \sum_{m=-l}^{l} \sum_{P=E,H} a_{lm}^{+P} (a_{lm}^{0P*} + a_{lm}^{+P*}). \tag{51}$$

Our results are shown in Fig. 6, together with the corresponding ATA results for comparison. In both approximations the absorbance is essentially determined by the dipole terms. However, while the ATA scatterer is characterized by a diagonal matrix $\langle \mathbf{T} \rangle$ with the same matrix elements for all values of m of given l ($-l \leq m \leq l$), this is not the case for the CPA scatterer. As shown by our calculation, the nondiagonal elements of the CPA $\langle \mathbf{T} \rangle$ matrix do not contribute significantly to absorption. However, the diagonal elements of the CPA $\langle \mathbf{T} \rangle$ matrix, of given l, are different for the different values of m, as demonstrated in Fig. 7. It is seen in this figure that the $lm = 11$ element of the CPA $\langle \mathbf{T} \rangle$ matrix ex-

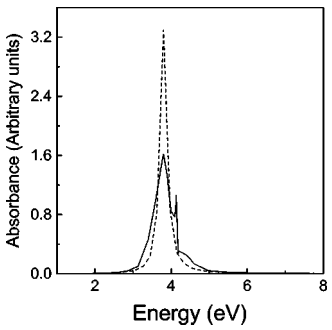

FIG. 6. Absorbance of light by a single CPA (solid line) and ATA (dashed line) effective scatterer for the system described in the caption of Fig. 5.

hibits an additional resonance at $\hbar\omega \cong 4.13$ eV, which does not occur in the ATA $\langle \mathbf{T} \rangle$ matrix. This resonance gives the second peak in the CPA absorbance curve of Fig. 6, which is also manifested in the absorbance of the disordered slab (see Fig. 5) as calculated by the CPA, and which is not obtained by the ATA.

In this respect the results for the thick slab we are considering here, differ markedly from those we obtained for a very thin slab consisting of a single layer of Drude spheres randomly distributed on a square lattice.[15] In that case, we have found that disorder produces a considerable shift and broadening of the resonance (and therefore of the corresponding absorbance peak) excited by an electric-field component parallel to the plane of spheres. The reason for this difference between the single layer of spheres and a slab of many layers of spheres appears to be the following. In the case of a single layer of spheres occupying a fraction of the sites of a 2D lattice, a dipole (say at the origin of coordinates) oscillating in the direction of the field (say the x direction) interacts with neighboring dipoles also oscillating in the x direction, which may be centered along the x direction [as in Fig. 8(a)], *or* normal to it, along the y direction [as in Fig. 8(b)]. The coupling between the dipoles in the first case [Fig. 8(a)] is different from that in the second case [Fig. 8(b)], and this leads to a considerable shift and broadening of the peak for the partly occupied 2D array of spheres. In contrast, in the fully occupied 2D lattice the local field at the given site is a

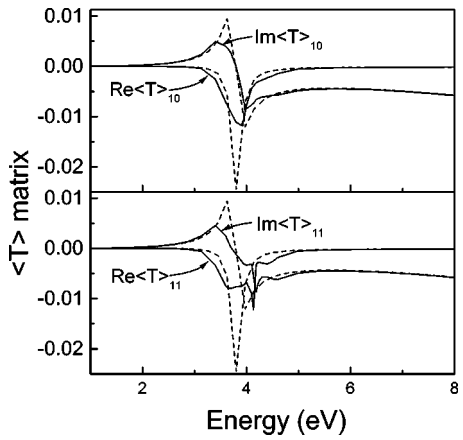

FIG. 7. Elements of the $\langle \mathbf{T} \rangle$ matrix corresponding to a CPA (solid lines) and an ATA (dashed lines) effective scatterer for the system described in the caption of Fig. 5.

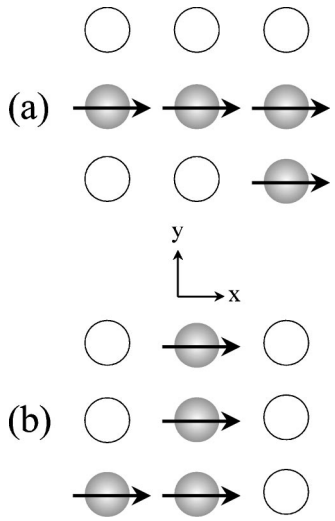

FIG. 8. Induced dipoles, indicated by arrows, in a partly occupied lattice. The empty circles denote nonoccupied sites.

uniquely determined quantity. In the ATA method the effect also disappears because we force the averaging on the system (see above). In the CPA treatment the effect is not averaged out, because of the way the $\langle \mathbf{T} \rangle$ matrix is constructed.[18] Now it appears that in the thick slab, the presence of the layers above and below a given layer, renders the distinction between the cases of Fig. 8(a) and Fig. 8(b) unprofitable, in the sense that both are likely to occur simultaneously in the partly occupied 3D lattice producing a local field at a given site which is more or less the same as that of a fully occupied lattice. This interpretation accords with the fact that the MG formula [Eq. (49)] produces practically the same results with the exact calculation for small volume fractions [in which case higher-multipole ($l>1$) bands are not important]. In this respect our results appear to confirm an assumption made by several authors,[33–35] but criticized by others,[22] namely that the MG equation describes reasonably well periodic and nearly periodic structures.

Finally, we must say something about the relation of the above model results to actual experiments. A metallic particle is not accurately described by a plasma sphere, its dielectric function will in general be more complicated than that of Eq. (47). By choosing appropriately the parameters ω_p and τ in Eq. (47), one should be able to reproduce the lower-frequency peak of the absorbance curve, but the remaining peaks (whether dipolar or multipolar in origin) will depend to a lesser or greater degree on the details of the dielectric function. The shape, or rather the distribution of sizes and shapes of the metallic particles in a given system will also affect the details of the absorbance curve. One must also remember that the absorption versus frequency curve, for light incident on a slab of the material depends, in general, on the thickness of the slab (see Fig. 7 of Ref. 32). In particular: one must not assume, as it is often done, that a peak in the absorbance curve coincides with a corresponding peak in the absorption coefficient defined by $\beta(\omega) = 2(\omega/c)\mathrm{Im}\sqrt{\epsilon(\omega)}$. This may or may not be the case. In summary, while our results support the view that disorder does not greatly affect the absorbance of a thick slab, in contrast to the situation of a very thin slab, they cannot be compared directly with any set of experimental data.

*Electronic address: vyannop@cc.uoa.gr

[1] J. D. Joannopoulos, R. D. Meade, and J. N. Winn, *Photonic Crystals* (Princeton University Press, New York, 1995).
[2] *Photonic Band Gap Materials*, edited by C. M. Soukoulis (Kluwer Academic, Dordrecht, 1996).
[3] E. Yablonovitch, Phys. Rev. Lett. **58**, 2058 (1987).
[4] A. J. Sievers, *Solar Energy Conversion*, edited by B. O. Seraphin (Springer, Berlin, 1979) p.57.
[5] F. Abelès, Y. Borensztein, and T. López-Rios, *Festkörperprobleme (Advances in Solid State Physics)* Vol. 24 (Braunschweig, Vieweg, 1984), p. 93.
[6] C. G. Granqvist and V. Wittwer, Sol. Energy Mater. Sol. Cells **54**, 39 (1998).
[7] R. Joerger, R. Gampp, A. Heinzel, W. Graf, M. Köhl, P. Gantenbein, and P. Oelhafen, Sol. Energy Mater. Sol. Cells **54**, 351 (1998).
[8] K. M. Leung and Y. F. Liu, Phys. Rev. Lett. **65**, 2646 (1990).
[9] N. Stefanou, V. Karathanos, and A. Modinos, J. Phys.: Condens. Matter **4**, 7389 (1992).
[10] J. B. Pendry and A. MacKinnon, Phys. Rev. Lett. **69**, 2772 (1992).
[11] K. Ohtaka and Y. Tanabe, J. Phys. Soc. Jpn. **65**, 2276 (1996).
[12] J. D. Joannopoulos, P. R. Villeneuve, and S. Fan, Solid State Commun. **102**, 165 (1997).
[13] I. I. Tarhan and G. H. Watson, Phys. Rev. Lett. **76**, 315 (1996).
[14] U. Kreibig, A. Althoff, and H. Pressmann, Surf. Sci. **106**, 308 (1981).
[15] N. Stefanou and A. Modinos, J. Phys.: Condens. Matter **5**, 8859 (1993).
[16] H. Y. Ryu, J. K. Hwang, and Y. H. Lee, Phys. Rev. B **59**, 5463 (1999).
[17] W. Lamb, D. M. Wood, and N. W. Ashcroft, Phys. Rev. B **21**, 2248 (1980).
[18] P. Soven, Phys. Rev. **156**, 809 (1967).
[19] B. L. Györffy and G. M. Stocks, *Electrons in Disordered Metals and at Metallic Surfaces*, edited by P. Phariseau, B. L. Györffy, and L. Scheire (Plenum, New York, 1979) p. 89.
[20] A. Gonis, *Green Functions for Ordered and Disordered Systems* (North-Holland, Amsterdam, 1992)
[21] B. N. J. Persson and A. Liebsch, Phys. Rev. B **28**, 4247 (1983).
[22] A. Liebsch and B. N. J. Persson, J. Phys. C **16**, 5375 (1983).
[23] N. Stefanou, V. Yannopapas, and A. Modinos, Comput. Phys. Commun. **113**, 49 (1998).
[24] A. Modinos, Physica A **141**, 575 (1987).
[25] K. Ohtaka, Phys. Rev. B **19**, 5057 (1979); J. Phys. C: Solid St. Phys. **13**, 667 (1980).
[26] J. L. Beeby, Proc. R. Soc. London, Ser. A **279**, 82 (1964).
[27] V. Eyert, J. Comput. Phys. **124**, 271 (1996).
[28] M. Abramowitz and I. A. Stegun, *Handbook of Mathematical Functions* (Dover, New York, 1965).
[29] S. L. Cunningham, Phys. Rev. B **10**, 4988 (1974).
[30] H. J. Monkhorst and J. D. Pack, Phys. Rev. B **13**, 5188 (1976).
[31] J. P. Dekker, A. L. Lodder, R. Zeller, and A. F. Tatarchenko, Solid State Commun. **97**, 1013 (1996).
[32] V. Yannopapas, A. Modinos, and N. Stefanou, Phys. Rev. B **60**, 5359 (1999).
[33] J. D. Jackson, *Classical Electrodynamics* (Wiley, New York, 1975).
[34] M. Kerker, *The Scattering of Light and Other Electromagnetic Radiation* (Academic Press, New York, 1969).
[35] M. Born and E. Wolf, *Principles of Optics* (Pergamon, Oxford, 1970).